HIGH ORDER SUBSYNCHRONOUS RESONANCE MODELS AND MULTI-MODE STABILIZATION

by

King Kui Tse

B.Sc. (Hon.), Northeastern University, 1974

A THESIS SUBMITTED IN PARTIAL FULFILMENT OF

THE REQUIREMENTS FOR THE DEGREE OF

MASTER OF APPLIED SCIENCE

in

THE FACULTY OF GRADUATE STUDIES

in the Department

of

Electrical Engineering

We accept this thesis as conforming to

the required standard

THE UNIVERSITY OF BRITISH COLUMBIA

June 1977

In presenting this thesis in partial fulfilment of the requirements for an advanced degree at the University of British Columbia, I agree that the Library shall make it freely available for reference and study. I further agree that permission for extensive copying of this thesis for scholarly purposes may be granted by the Head of my Department or by his representatives. It is understood that copying or publication of this thesis for financial gain shall not be allowed without my written permission.

Department of Electrical Engineering

The University of British Columbia
2075 Wesbrook Place
Vancouver, Canada
V6T 1W5

Date July 6, 1977.

6

ABSTRACT

Subsynchronous resonance (SSR) occurs in a series-capacitor-compensated power system when a mechanical mass-spring mode coincides with that of the electrical system. In this thesis, a complete high order model including mass-spring system, series-capacitor-compensated transmission line, synchronous generator, turbines and governors, exciter and voltage regulator is derived. Eigenvalue analysis is used to find the effect of capacitor compensation, conventional lead-lag stabilizer, loading and dampers on SSR. Finally, controllers are designed to stabilize multi-mode subsynchronous resonance simultaneously over a wide range of capacitor compensation.

TABLE OF CONTENTS

Page

LIST OF TABLES

LIST OF ILLUSTRATIONS

ACKNOWLEDGEMENT

I wish to express my sincere gratitude to my supervisors, Dr. Y.N. Yu and Dr. M.D. Wvong, for their patience, guidance, many hours of consultation and valuzble advice during the course of the research work and writing of this thesis.

Financial support from a British Columbia Telephone Company Scholarship, a University of British Columbia Summer Research Fellowship and a teaching assistantship is gratefully acknowledged.

Thanks are also due to Mary Ellen Flanagan and Sannifer Louie for typing this thesis.

I am grateful to my parents and Mui Ha in Hong Kong for their patient understanding and encouragement throughout my university career.

=NOMENCLATURE

General

X	state vector of unmeasurable model
Z	state vector of measurable model
Y	state vector of canonical
A	system matrix of X-model
F	system matrix of Z-model
F_o	system matrix of Y-model
B	control matrix of X-model
G	control matrix of Z-model
G_o	control matrix of Y-model
U	control vector
M	transformation matrix for Z-model
T	transformation matrix for Y-model
λ	eigenvalue
j	complex operator, $\sqrt{-1}$

Mass-Spring System

M	inertia coefficient = 2H
H	inertia constant
K	shaft stiffness
D	damping
θ	rotor angle
ω	rotor speed
ω_o	synchronous speed

Synchronous Machine

i	instantaneous value of current
V	instantaneous value of voltage

ψ	flux-linkage
R	resistance
X	reactance
δ	torque angle, rad.
ω	angular velocity, rad./s
T_e	electrical torque
i_t	terminal voltage
P+jQ	generator output power

<u>Transmission Network</u>

X_t, R_t	reactance and resistance of transformer
X_e, R_e	reactance and resistance of the line
X_c	reactance of capacitor
V_o	infinite bus voltage

<u>Exciter and Voltage Regulator</u>

K_A	regulator gain
T_A	regulator time constant, s
T_E	exciter time constant, s
$V_{ref.}$	reference voltage

<u>Governor and Turbine System</u>

K_g	actuator gain
T_1, T_2	actuator time constant
T_3	servomotor time constant
a	change in actuator signal
P_{GV}	power at gate outlet
T_{CH}	steam chest time constant
T_{RH}	reheater time constant
T_{CO}	cross-over time constant

F_{HP}	high pressure turbine power fraction
F_{IP}	intermediate pressure turbine power fraction
F_{LP1}	low pressure turbine 1 power fraction
F_{LP2}	low pressure turbine 2 power fraction
T_{HP}	high pressure turbine torque
T_{IP}	intermediate pressure turbine torque
T_{LP1}, T_{LP2}	low pressure turbine torque

Subscripts

d,q	direct- and quadrature-axis stator quantities
f	field circuit quantities
D,Q,G	direct- and quadrature-axis damper quantities
c	quantities associate with capacitor
a	armature phase quantities

Superscripts

-1	inverse of a matrix
t	transpose of a matrix
•	differential operator

Prefix

Δ	linearized quantities
s	differential operator
p	differential operator

1. INTRODUCTION

1.1 Subsynchronous Resonance [1]

To increase the power transfer capability of a power system, the use of series-capacitor-compensated transmission lines is the best alternative to the addition of transmission lines because of environmental considerations and the limited availability of right-of-way. They are also more economical than other methods such as HVDC. However, subsynchronous resonance (SSR) may occur and shaft damage may result. Two turbine shafts were severely damaged [2] at the Mohave generating station of the Southern California Edison Company because of the excessive torsional oscillations caused by interaction between the electrical resonance of the series-capacitor-compensated system and the natural modes of the multi-mass generator turbine mechanical system.

Subsynchronous resonance may occur in a system in the steady-state or transient state due to a system fault or major switching. The former may be called the steady-state subsynchronous resonance and the latter the transient subsynchronous resonance. The main problems are the self excitation, the torsional interaction, and the transient torques [3]. When SSR occurs, the synchronous machine is self-excited and behaves like an induction generator. If the negative resistance of the machine, as an induction generator, exceeds the total resistance of the external electrical system, self excitation of SSR occurs.

Torsional oscillation is due to the mechanical modes of the multi-mass turbine-generator system. The torsional frequencies are in the subsynchronous range. If the electrical resonant frequency is equal or close to a torsional mode, the rotor oscillations and the induced voltages will build up and the interaction between the electrical and mechanical systems ensues [1,4].

Transient torques are caused by system disturbances on a series-capacitor-compensated line and the energy stored in the series capacitor produces large subsynchronous currents in the lines. When the frequency of the current coincides with the natural torsional frequency, transient torque results.

After the reported turbine shaft failures [3], corrective measures have been proposed. Some of them are under serious consideration and others already put into practice. Without too much modification to the existing system, the simplest way to avoid the subsynchronous resonance is to reduce the degree of capacitor compensation. Another suggestion is the installation of passive filter units in series with the generator transformer neutral at the high voltage side. Each filter unit is a high-Q parallel resonant circuit tuned to block the subsynchronous current at a particular frequency corresponding to one of the mechanical modes. Additional amortisseur windings on the pole faces can reduce the effective negative resistance [5]. Supplementary excitation control is being considered and the stabilizing signals are derived from rotor speed. Finally a subsynchronous overcurrent relay has been developed for the automatic protection of generating units in case of sustained subsynchronous oscillations.

1.2 Scope of the thesis

The widely accepted method for subsynchronous resonance studies in engineering practice consists of a two-step analysis [5]. The electrical and mechanical modes are determined separately. The transient electrical torque from the electrical system is calculated first and then applied to the mechanical system as a forcing function. In this thesis, a complete model including the electrical, mechanical and control systems will be developed and presented in Chapter 2. By using eigenvalue analysis, the effect of various degrees of compensation, loading conditions and conventional supplementary excitation control on subsynchronous resonance will be examined in Chapter 3. For broad-band frequency multi-mode subsynchronous resonance control, linear optimal controllers will be designed in Chapter 4. A summary of all important results and conclusions will be presented in Chapter 5.

2. A COMPLETE POWER SYSTEM MODEL FOR SUBSYNCHRONOUS RESONANCE STUDIES

2.1 Introduction

For any dynamic or transient stability study of a power system, an accurate model of the system is required. In addition to the individual efforts [2,7,12], a benchmark model has been proposed by the IEEE Subsynchronous Resonance Working Group for SSR studies [20]. In this chapter, a complete subsynchronous resonance model is presented, including steam turbines and generator multi-mass torsional system, the turbine torques and speed governor, the synchronous generator, the capacitor-compensated transmission lines, and the exciter and voltage regulator. A functional block diagram of the complete system is shown in Fig. 2-1.

2.2 The Steam Turbines and Generator Multi-Mass Torsional System

Assume that the steam turbine-generator set consists of one high-pressure steam turbine, one intermediate-pressure turbine, two low-pressure turbines, one generator rotor and one exciter, all mechanically coupled on the same shaft as shown in Fig. 2-2. They comprise a six-mass torsional system. For the purpose of analysis [13], they are considered to have concentrated masses and to be coupled by shafts of negligible mass and known torsional stiffness. Each mass is denoted by a circular disc, as in Fig. 2-3, with an inertia constant M_i, a positive torsional torque $K_i(\theta_{i+1} - \theta_i)$ on the left and a negative torque $-K_{i-1}(\theta_i - \theta_{i-1})$ on the right. There is an external torque T_i applied to the mass in a positive direction, an accelerating torque $M_i\dot{\omega}_i$ in the same direction and a damping torque $D_i\omega_i$ in the opposite direction. The net accelerating torque becomes

$$M_i\dot{\omega}_i = T_i - D_i\omega_i + K_i(\theta_{i+1} - \theta_i) - K_{i-1}(\theta_i - \theta_{i-1}) \qquad (2\text{-}1)$$

where M_i = the inertia constant of i^{th} rotor

θ_i = the rotational displacement for i^{th} rotor

D_i = damping coefficient for i^{th} rotor

$K_{i,i+1}$ = the torsional stiffness of the shaft between the i^{th} rotor and the $i+1^{th}$ rotor

By applying equation (2-1) to the six mass turbine-generator system, twelve differential equations are obtained:

High Pressure
$$p\omega_6 = \frac{K_{56}}{M_6}\theta_5 - \frac{K_{56}}{M_6}\theta_6 - \frac{D_{66}}{M_6}\omega_6 + \frac{T_{HP}}{M_6} \quad (2\text{-}2)$$

$$p\theta_6 = \omega_6\ \omega o \quad (2\text{-}3)$$

Intermediate Pressure
$$p\omega_5 = \frac{K_{56}}{M_5}\theta_6 - \frac{(K_{45}+K_{56})}{M_5}\theta_5 + \frac{K_{45}}{M_5}\theta_4 - \frac{D_{55}}{M_5}\omega_5 + \frac{T_{IP}}{M_5} \quad (2\text{-}4)$$

$$p\theta_5 = \omega_5\ \omega o \quad (2\text{-}5)$$

Low Pressure 1
$$p\omega_4 = \frac{K_{45}}{M_4}\theta_5 - \frac{(K_{34}+K_{45})}{M_4}\theta_4 + \frac{K_{34}}{M_4}\theta_3 - \frac{D_{44}}{M_4}\omega_4 + \frac{T_{LP1}}{M_4} \quad (2\text{-}6)$$

$$p\theta_4 = \omega_4\ \omega o \quad (2\text{-}7)$$

Low Pressure 2
$$p\omega_3 = \frac{K_{34}}{M_3}\theta_4 - \frac{(K_{23}+K_{34})}{M_3}\theta_3 + \frac{K_{23}}{M_3}\delta - \frac{D_{33}}{M_3}\omega 3 + \frac{T_{LP2}}{M_3} \quad (2\text{-}8)$$

$$p\theta_3 = \omega_3\ \omega o \quad (2\text{-}9)$$

Generator
$$p\ \omega = \frac{K_{23}}{M_2}\theta_3 - \frac{(K_{12}+K_{23})}{M_2}\delta + \frac{K_{12}}{M_2}\theta_1 - \frac{D_{22}}{M_2}\omega - \frac{Te}{M_2} \quad (2\text{-}10)$$

$$p\ \delta = \omega\ \omega o \quad (2\text{-}11)$$

Exciter
$$p\omega_1 = \frac{K_{12}}{M_1}\delta - \frac{K_{12}}{M_1}\theta_1 - \frac{D_{11}}{M_1}\omega_1 \quad (2\text{-}12)$$

$$p\theta_1 = \omega_1\ \omega o \quad (2\text{-}13)$$

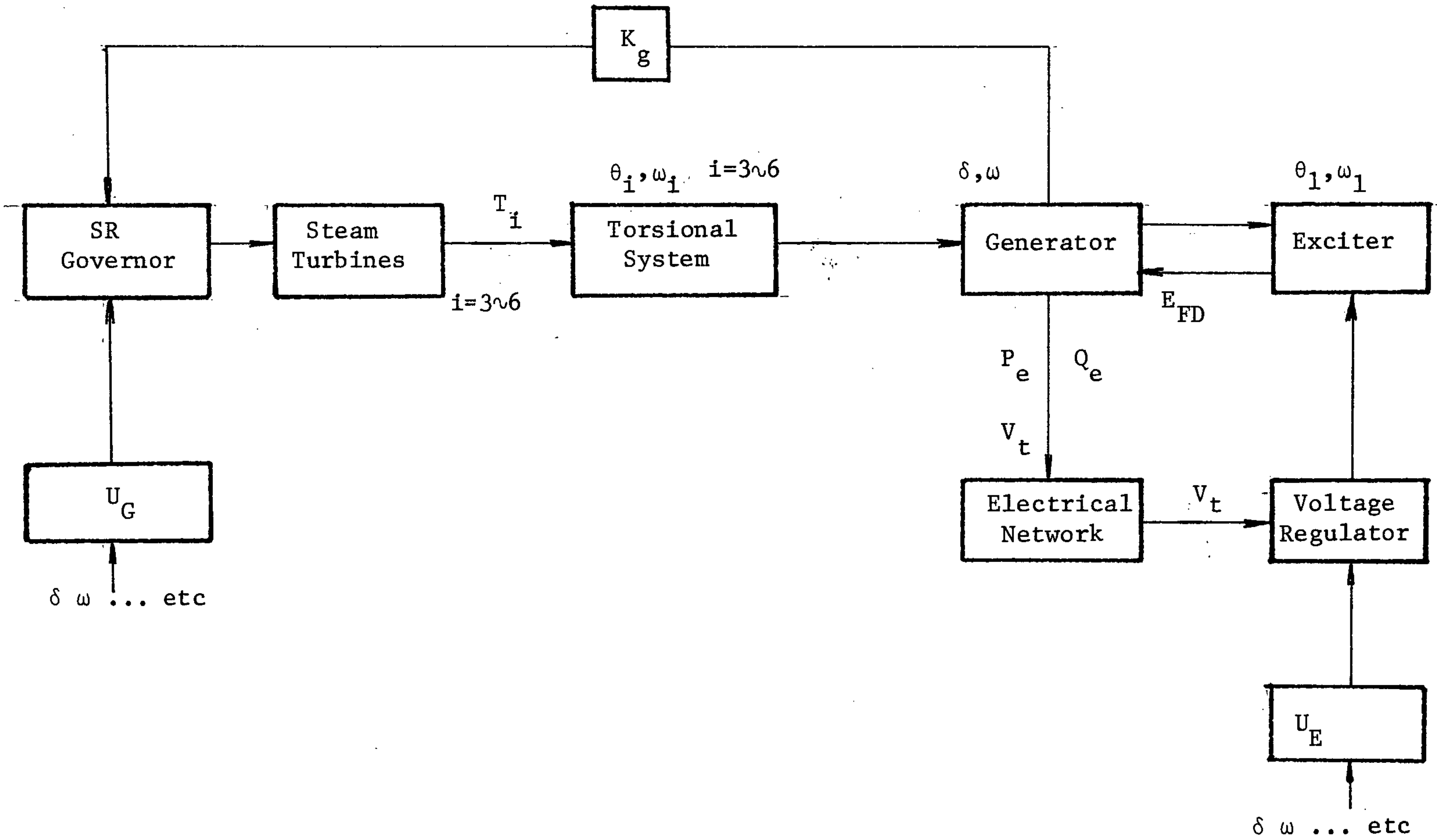

Fig. 2-1 A functional block diagram of the complete system for subsynchronous resonance studies.

The generator has an electric torque output Te, and the exciter electric torque is neglected. Note that while angles are in radians, the speed is in p.u.;

$$\omega o = 1 \text{ p.u.} = 377 \text{ electrical radian/second}$$

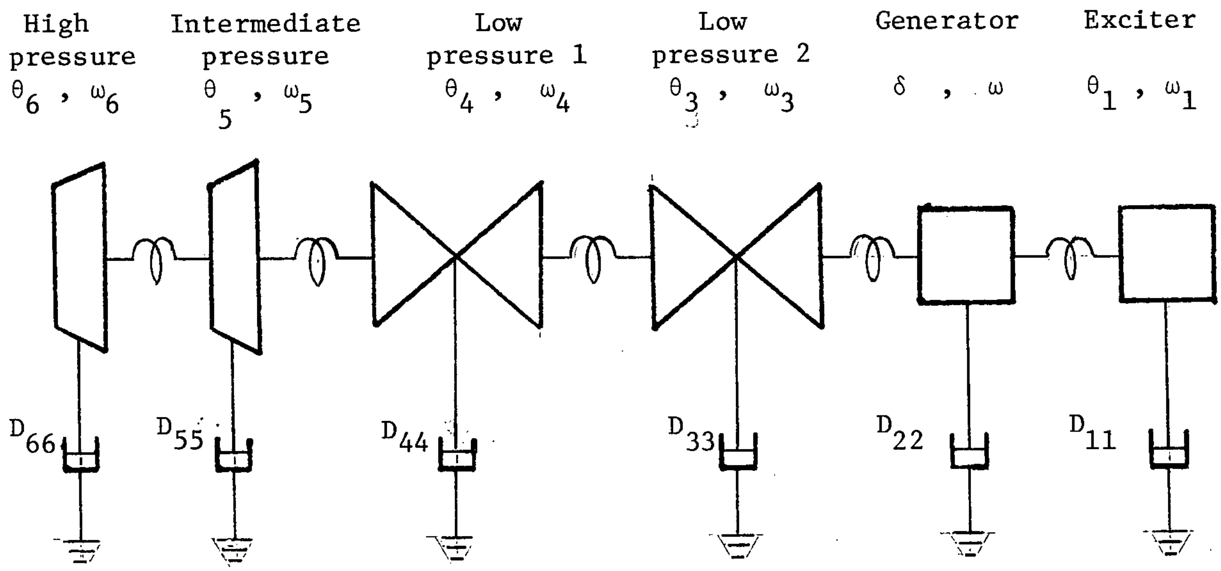

Fig. 2-2 Mechanical mass and shaft system

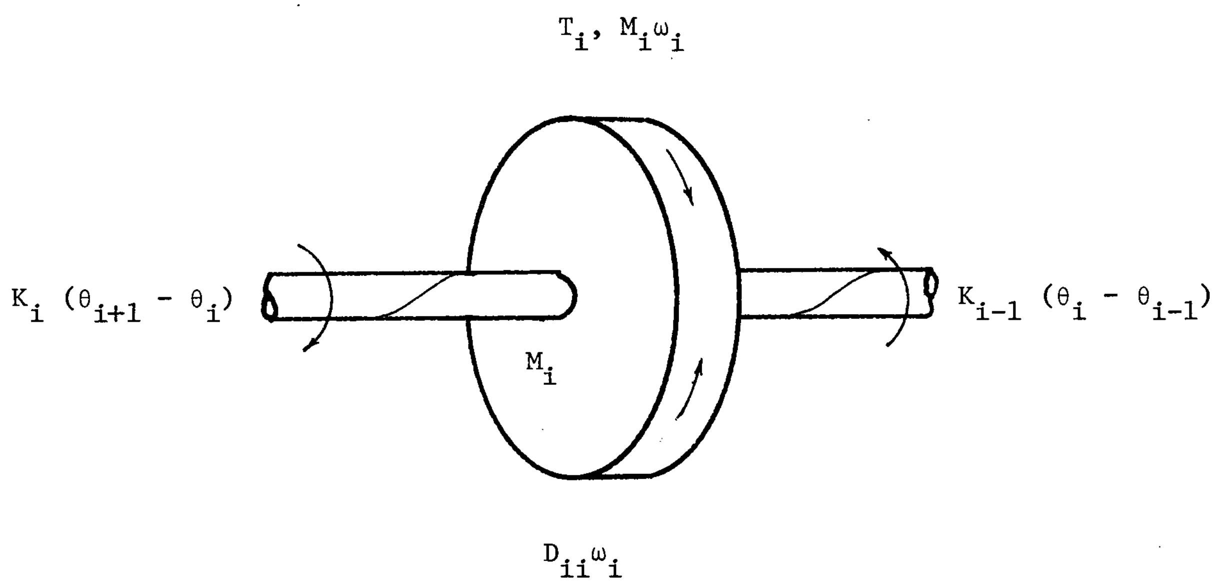

Fig. 2-3 Torques of a mass-shaft system

2.3 The Turbine Torques and Speed Governor

The steam turbine and speed governor representation is based on an IEEE committee report [14]. Usually the speed is sensed between the low-pressure turbine and the generator rotor. Combined with the speed reference, the speed deviation or error signal is derived and relayed through the actuator to activate the servomotor, which in turn opens or closes the steam valves. A block diagram [14] is shown in Fig. 2-4. For a linear study, the system equations may be written;

$$p\,\Delta a = \frac{K_g}{T_1}\Delta\omega - \frac{1}{T_1}\Delta a \qquad (2\text{-}14)$$

$$p\,\Delta P_{GV} = \frac{1}{T_3}\Delta a - \frac{1}{T_3}\Delta P_{GV} \qquad (2\text{-}15)$$

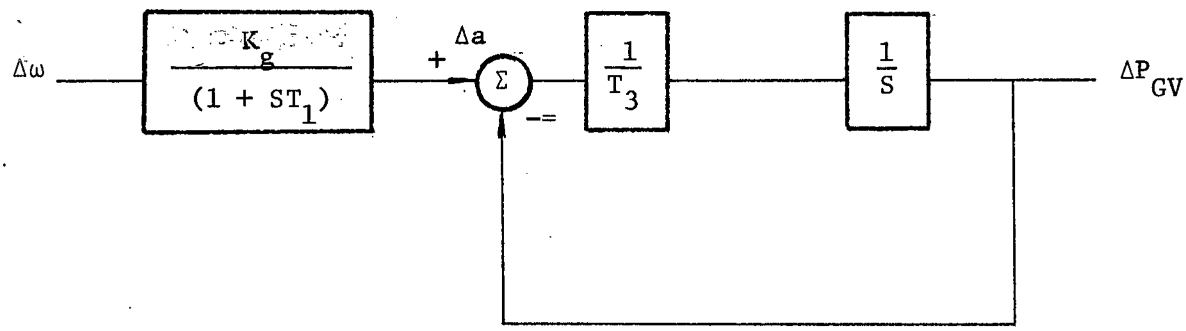

Fig. 2-4 A speed governor model for the steam turbine system

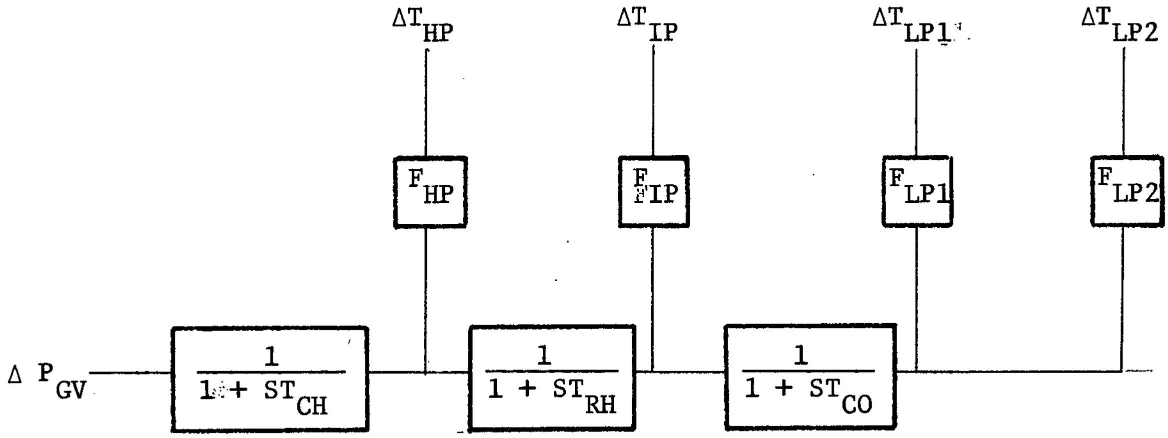

Fig. 2-5 A Linear model of the steam turbine system

Fig. 2-5 shows a standard turbine representation for stability studies [14]. The system consists of one high-pressure, one intermediate-pressure and two low-pressure turbines. Their output torques are denoted by T_{HP}, T_{IP}, T_{LP1}, T_{LP2}, respectively. There is a reheater between high-pressure and intermediate-pressure stages, and crossover pipings between intermediate-pressure and low-pressure stages. The steam into the turbines flow through the governor-controlled valves at the inlet of the steam chest. The time constants of the steam chest, the reheater and the cross-over piping are denoted by T_{CH}, T_{RH}, and T_{CO}, respectively. F_{HP}, F_{IP}, F_{LP1}, and F_{LP2} represent fractions of the total power developed in the various stages. Therefore

$$p \, \Delta T_{HP} = \frac{F_{HP}}{T_{CH}} \Delta P_{GV} - \frac{1}{T_{CH}} \Delta T_{HP} \tag{2-16}$$

$$p \, \Delta T_{IP} = \frac{F_{IP}}{F_{HP} \times T_{RH}} \Delta T_{HP} - \frac{1}{T_{RH}} \Delta T_{IP} \tag{2-17}$$

$$p \, \Delta T_{LP1} = \frac{F_{LP1}}{F_{IP} \times T_{CO}} \Delta T_{IP} - \frac{1}{T_{CO}} \Delta T_{LP1} \tag{2-18}$$

$$\Delta T_{PL2} = \frac{F_{LP2}}{F_{LP1}} \Delta T_{LP1} \tag{2-19}$$

2.4 The Synchronous Generator

The synchronous generator is assumed to have six windings. In addition to the d and q armature windings on the respective axes, there is a field winding f, a damper winding D on the d-axis and two damper windings Q and G on the q-axis. They are schematically shown in Fig. 2-6.

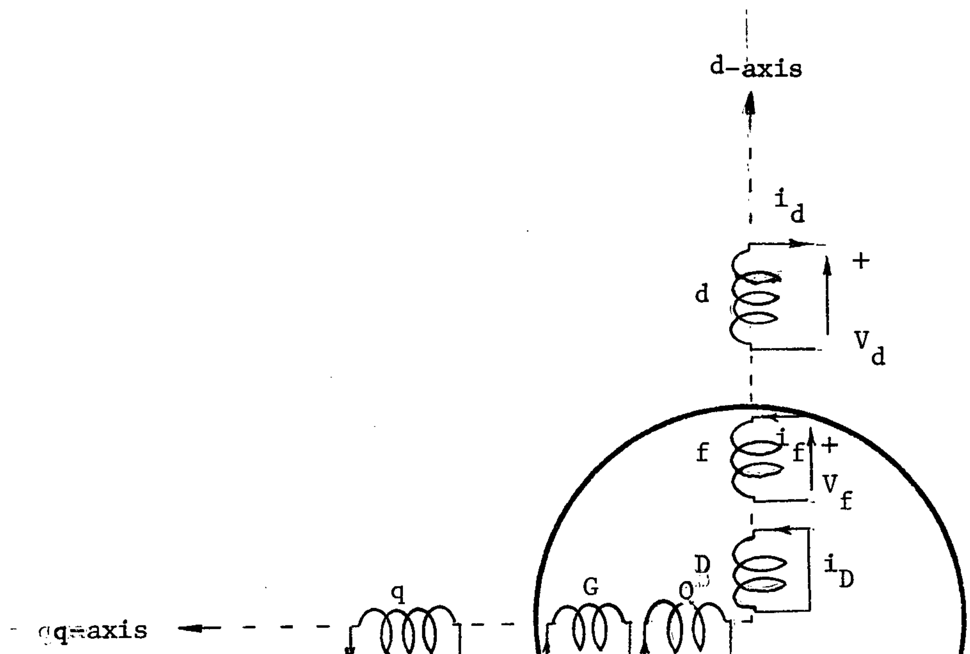

Fig. 2-6 A synchronous machine model

The voltage equations in the linear form are

$$\Delta V_d = p\Delta\psi_d - \omega o\Delta\psi_q - \psi_{qo}\Delta\omega - R_a\Delta i_d$$

$$\Delta V_q = p\Delta\psi_q + \omega o\Delta\psi_d + \psi_{do}\Delta\omega - R_a\Delta i_q$$

$$\Delta V_f = p\Delta\psi_f + R_f \Delta i_f$$

$$0 = p\Delta\psi_D + R_D \Delta i_D$$

$$0 = p\Delta\psi_Q + R_Q \Delta i_Q$$

$$0 = p\Delta\psi_G + R_G \Delta i_G \qquad (2\text{-}20)$$

where the flux linkages are

$$\begin{bmatrix} \Delta\psi_d \\ \Delta\psi_q \\ \Delta\psi_f \\ \Delta\psi_D \\ \Delta\psi_Q \\ \Delta\psi_G \end{bmatrix} = \frac{1}{\omega o} \begin{bmatrix} -X_d & 0 & X_{ad} & X_{ad} & 0 & 0 \\ 0 & -X_q & 0 & 0 & X_{aq} & X_{aq} \\ -X_{ad} & 0 & X_f & X_{ad} & 0 & 0 \\ -X_{ad} & 0 & X_{ad} & X_D & 0 & 0 \\ 0 & -X_{aq} & 0 & 0 & X_Q & X_{aq} \\ 0 & -X_{aq} & 0 & 0 & X_{aq} & X_G \end{bmatrix} \begin{bmatrix} \Delta i_d \\ \Delta i_q \\ \Delta i_f \\ \Delta i_D \\ \Delta i_Q \\ \Delta i_G \end{bmatrix} \qquad (2\text{-}21)$$

and the ψ's, X's, R's and i's are the per unit flux linkages, reactances, resistances and currents respectively.

The saturation in the iron circuit is neglected. The stator transient voltages $p\psi_d$ an $p\psi_q$, although normally neglected in stability studies [15,16] are retained in this study because the capacitor compensated transmission lines, to which the armature windings are connected in series, must be described by differential equations.

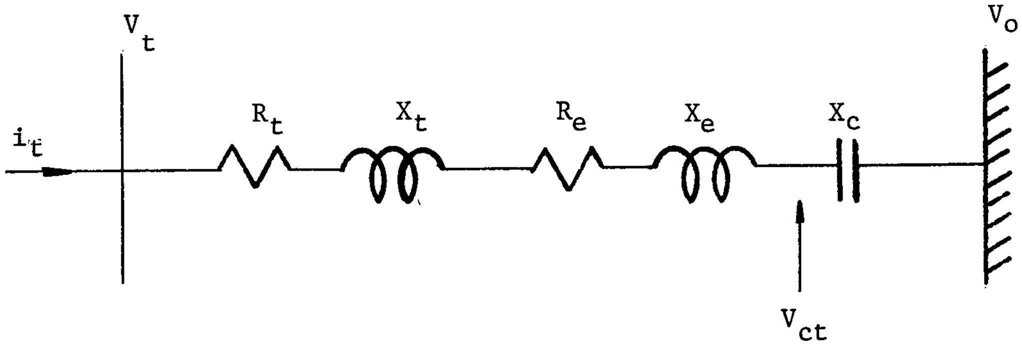

Fig. 2-7 A single line representation of the transmission line

In Fig. 2-7, V_d and V_q are d-q components of the terminal voltage V_c is the voltage across the capacitor and V_{ct} is the terminal voltage at the capacitor. The transformer is represented by a reactance X_t and a resistance R_t and the transmission line by a reactance X_e and a line resistance R_e.

Let the terminal voltage equations in a-b-c phase coordinates be

$$[V_t]_{a,b,c} = [R]\,[I_t]_{a,b,c} + [L]\,\frac{d}{dt}\,[I_t]_{a,b,b} + [V_c]_{a,b,c} + [V_o]_{a,b,c} \qquad (2\text{-}22)$$

where $[R]$ = a resistance matrix: $R_t + R_e$

$[L]$ = an inductance matrix: $\dfrac{X_t + X_e}{\omega o}$

Let Park's transformation matrix be

$$[T] = \begin{array}{c} \\ a \\ b \\ c \end{array} \begin{array}{c} \begin{array}{ccc} d & q & o \end{array} \\ \begin{bmatrix} \cos\theta & -\sin\theta & 1 \\ \cos(\theta-120) & -\sin(\theta-120) & 1 \\ \cos(\theta+120) & -\sin(\theta+120) & 1 \end{bmatrix} \end{array} \qquad (2\text{-}23)$$

and the transformations are

$$[V]_{a,b,c} = [T][V]_{d,q,o} \quad \text{and} \quad [I]_{a,b,c} = [T][I]_{d,q,o} \tag{2-24}$$

Then we have

$$[V]_{d,q,o} = [R][I]_{d,q,o} + [L]\frac{d}{dt}[I]_{d,q,o} + [L][T]^{-1}\frac{d}{dt}[T]\cdot[I]_{d,q,o}$$

$$+ [V_c]_{d,q,o} + [V_o]_{d,q,o} \tag{2-25}$$

Note that

$$[T]^{-1}\frac{d}{dt}[T] = \begin{bmatrix} 0 & -1 & 0 \\ 1 & 0 & 0 \\ 0 & 0 & 1 \end{bmatrix} \frac{d\theta}{dt} \tag{2-26}$$

The terminal voltage equation in d-q coordinates when linearized, becomes

$$\begin{bmatrix} \Delta V_d \\ \Delta V_q \end{bmatrix} = \begin{bmatrix} R_t+R_e & -X_t-X_e \\ X_t+X_e & R_t+R_e \end{bmatrix} \begin{bmatrix} \Delta i_d \\ \Delta i_q \end{bmatrix} + \frac{(X_t+X_e)}{\omega_o} p \begin{bmatrix} \Delta i_d \\ \Delta i_q \end{bmatrix} + \begin{bmatrix} \Delta V_{cd} \\ \Delta V_{cq} \end{bmatrix} + \begin{bmatrix} V_o \cos\delta_o \\ -V_o \sin\delta_o \end{bmatrix} \Delta\delta \tag{2-27}$$

where V_{cd} and V_{cq} are the d-q components of the voltage across the capacitor, and V_o the infinite bus voltage. The zero component equation is orthogonal to the other two equations and is usually neglected except for asymmetric loading. The capacitor equations may be written

$$[I]_{a,b,c} = [C]\frac{d}{dt}[V_c]_{a,b,c} \tag{2-28}$$

After transformation, it becomes

$$[I]_{d,q,o} = [C]\frac{d}{dt}[V_c]_{d,q,o} + [C][T]^{-1}\frac{d}{dt}[T][V_c]_{d,q,o} \tag{2-29}$$

which when linearized, gives

$$\begin{bmatrix} \Delta I_d \\ \Delta I_q \end{bmatrix} = \frac{1}{\omega_o X_c} p \begin{bmatrix} \Delta V_{cd} \\ \Delta V_{cq} \end{bmatrix} + \frac{1}{X_c} \begin{bmatrix} -\Delta V_{cq} \\ \Delta V_{cd} \end{bmatrix} \tag{2-30}$$

2.5 The Exciter and Voltage Regulator

The exciter and voltage regulator model in this thesis is based on an IEEE committee report [18] with some simplification. The regulator input filter time constant, the saturation function and the stabilizing feedback loop are neglected.

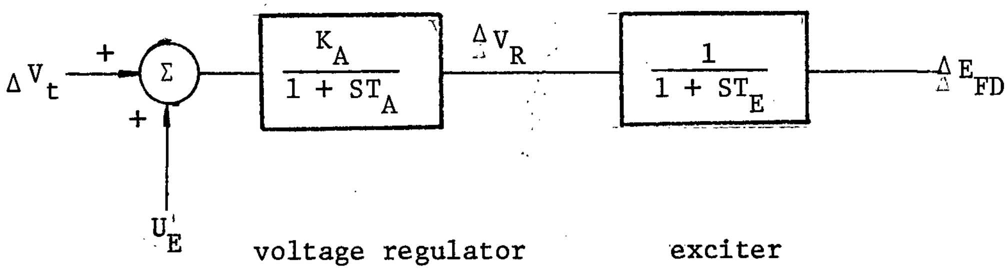

Fig. 2-8 Exciter and Voltage Regulator Model

In Fig. 2-8, V_t is the generator terminal voltage, U_E the supplementary control, K_A the voltage regulator gain, T_A its time constant, T_E the exciter time constant and E_{FD} a per unit output voltage of the exciter. Although the voltage limits are shown in the figure, they will be neglected in linear analysis. Mathematically we have

$$p\ \Delta V_R = \frac{K_A}{T_A} \Delta V_t + \frac{K_A}{T_A} u - \frac{1}{T_A} \Delta V_R \tag{2-31}$$

$$p\ \Delta E_{FD} = \frac{1}{T_E} \Delta V_R - \frac{1}{T_E} \Delta E_{FD} \tag{2-32}$$

where the linearized terminal voltage

$$\Delta V_t = \frac{V_{do}}{V_{to}} \Delta V_d + \frac{V_{qo}}{V_{to}} \Delta V_q \tag{2-33}$$

Substituting ΔV_d, ΔV_q from equation (2-27) into equation (2-33) and the results into equation (2-31), we have

$$p\,\Delta V_R = \frac{V_{do}K_A(X_t+X_e)}{V_{to}T_A\,\omega_o}\,p\,\Delta i_d + \frac{V_{qo}K_A(X_t+X_e)}{V_{to}T_A\,\omega\omega_o}\,p\,\Delta i_q + \frac{K_A V_{do}}{T_A V_{to}}\,\Delta V_{cd}$$

$$+ \frac{K_A V_{qo}}{T_A V_{to}}\,\Delta V_{cq} + \frac{K_A}{T_A\,V_{to}}\,[V_{do}(R_t+R_e) + V_{qo}\,(X_t+X_e)]\,\Delta i_d$$

$$+ \frac{K_A}{T_A V_{to}}\,[-V_{do}(X_t+X_e) + V_{qo}(R_t+R_e)]\,\Delta i_q + \frac{K_A}{T_A}\,\Delta u - \frac{1}{T_A}\,\Delta V_R$$

$$+ \frac{K_A V_o}{T_A V_{to}}\,[V_{do}\cos\delta_o - V_{qo}\sin\delta_o]\,\Delta\delta \qquad (2\text{-}34)$$

Fig. 2-9 shows a supplementary excitation control of the lead-lag compensation type [19].

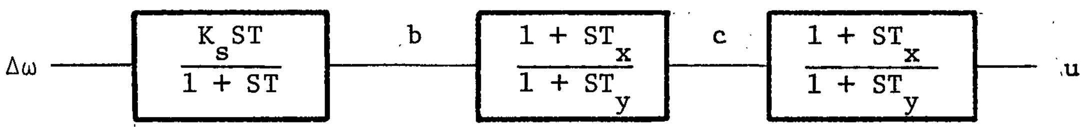

Fig. 2-9 A supplementary excitation control

Mathematically,

$$K_s\,T\,p\Delta\dot{\omega} - T\,p\quad b = \quad b \qquad (2\text{-}35)$$

$$T_x\,p\quad b - T_y\,p\quad c = \quad c - \quad b \qquad (2\text{-}36)$$

$$-T_y\,p\quad u + T_x\,p\quad c = \quad u - \quad c \qquad (2\text{-}37)$$

2.6 State Equations for the Complete System

The component system equations previously derived can be combined into a single set of state equations in the form of

$$\dot{\underline{X}} = [A]\ \underline{X} \qquad (2\text{-}38)$$

where $\underline{X}$ is the state variable vector and [A] the system matrix. Equation (2-38) can be conveniently partitioned

$$\begin{bmatrix} \dot{X}_I \\ \hdashline \dot{X}_{II} \end{bmatrix} = \begin{bmatrix} A_{I,\,I} & A_{I,\,II} \\ \hdashline A_{II,I} & A_{II,II} \end{bmatrix} \begin{bmatrix} X_I \\ \hdashline X_{II} \end{bmatrix} \qquad (2\text{-}39)$$

where X_I contains the state variables of the mechanical system and X_{II} those of the electrical system; namely

$X_I = [\omega_1, \theta_{11}, \omega, \delta, \omega_3, \theta_3, \omega_4, \theta_4, \omega_5, \theta_5, \omega_6, \theta_6, a, P_{GV}, T_{HP}, T_{IP}, T_{LP1}]$

$X_{II} = [i_d, i_q, i_f, i_D, i_Q, i_G, V_{cd}, V_{cq}, V_R, E_{FD}]$

$A_{I,II}$ represents the coupling between the two systems where the interaction occurs through the electrical torque T_e. Since

$$T_e = (\psi_d i_q - \psi_q i_d) \quad \text{per unit} \qquad (2\text{-}40)$$

$$\Delta T_e = \{ (\psi_{do}\,\Delta i_q + i_{qo}\Delta\psi_d - \psi_{qo}\Delta i_d - i_{do}\Delta\psi_q)\}/\omega_o$$

$$= \{ (X_q - X_d) i_{qo}\Delta i_d + [(X_q - X_d) i_{do} + X_{ad} i_{fo}]\,\Delta i_q + i_{qo} X_{ad}\Delta i_f$$

$$+ i_{qo} X_{ad}\,\Delta i_D - i_{do} X_{aq}\Delta i_Q - i_{do} X_{aq}\,\Delta i_G \} / \omega_o \qquad (2\text{-}41)$$

Next, the partitioned matrices $A_{II,I}$ and $A_{II,II}$ of the electrical system shall be first assembled in the form of

$$B\,\dot{X}_{II} = C_I\,X_I + C_{II}\,X_{II} \qquad (2\text{-}42)$$

Then we have

$$\dot{X}_{II} = B^{-1} C_I X_I + B^{-1} C_{II} X_{II} \tag{2-43}$$

or $$\dot{X}_{II} = A_{II,I} X_I + A_{II,II} X_{II}$$

where $$A_{II,I} = B^{-1} C_I \quad ; \quad A_{II,II} = B^{-1} C_{II} \tag{2-44}$$

Thus we have completed the derivation of the state equations for the overall system.

3. EIGENVALUE ANALYSIS OF THE SSR MODEL

3.1 Introduction

Eigenvalue analysis technique is useful in investigating the stability of systems. The complex eigenvalues are associated with oscillatory modes of the system and the real part of the eigenvalues provide the information on system damping. When an eigenvalue has a positive real part, instability of the system is indicated.

In this thesis the effect of capacitor compensation, conventional stabilizer and dampers will be investigated using the data taken from the benchmark model [20] Table 3-1.

3.2 The Effect of Capacitor Compensation

Fig. 3-1 and 3-2 show the eigenvalues of the system with various degrees of capacitor compensation, at a particular loading. The pair of eigenvalues corresponding to $\Delta\delta$ and $\Delta\omega$ of the synchronous machine have positive real parts when the compensation is 20% or less. The natural frequencies of the multi-mass torsional system are approximately 298, 203, 160, 127 and 99 radians/second which correspond to 47.4, 32.3, 25.5, 20.2, and 16 Hz respectively. By changing the degree of compensation, the natural oscillation frequency of the transmission system changes. When the frequency of the electrical mode is closedto a mechanical mode, SSR may occur. At 50% and 60% compensation, two mechanical modes are excited simultaneously.

3.3 The Effect of Conventional Stabilizer

Fig. 3-3 and 3-4 repeat the study of the effectoof capacitor compensation, but with the addition of a conventional stabilizer of the lead-lag type. Whereas the pair of eigenvalues corresponding to $\Delta\delta$ and

$\Delta\omega$ of the synchronous machine were unstable for compensation below 30%, Fig. 3-1 shows they are substantially moved to the left half of the complex plane with the supplementary excitation control, Fig. 3-3. However, the lowest mechanical mode of 99 rad/sec is always excited and shifted to the right-half plane. This is in agreement with other findings [21, 22]. The damping of other mechanical modes is decreased slightly.

3.4 The Effect of Loading

The effect of different loading with and without stabilizer on SSR is shown in Fig. 3-5 and 3-6 respectively. Most of the eigenvalues do not change except those corresponding to the generator mechanical model. Generally the system becomes more unstable with more leading power factor. Most utilities operate their systems between 0.9 power factor lagging and unity power factor. For this reason, 0.9 power factor lagging is chosen for the studies here.

3.5 The Effect of Dampers

As reported [5] the addition of an amortisseur winding can reduce the possibility of SSR. For this investigation, the additional damper effect is represented by decreased damper impedance. When the total reactance of line and transformer is zero, SSR occurs. The result is shown in Table 3-2. The excited mode is damped out by decreasing the damper impedance which agrees with previous results [5].

Table 3-1 Numerical Values of Model in p.u. system

Mass-spring System Parameters

$M_1 = 0.068433$	$K_{12} = 2.822$	$D_{11} = 0.1$
$M_2 = 1.736990$	$K_{23} = 70.858$	$D_{22} = 0.1$
$M_3 = 1.768430$	$K_{34} = 52.038$	$D_{33} = 0.1$
$M_4 = 1.717340$	$K_{45} = 34.929$	$D_{44} = 0.1$
$M_5 = 0.311178$	$K_{56} = 19.303$	$D_{55} = 0.1$
$M_6 = 0.185794$		$D_{66} = 0.1$

Synchronous Machine Parameters

$X_d = 1.79$	$X_f = 1.6999$	$R_f = 0.00105$
$X_{ad} = 1.66$	$X_D = 1.6657$	$R_D = 0.00371$
$X_q = 1.71$	$X_Q = 1.6845$	$R_Q = 0.00526$
$X_{aq} = 1.58$	$X_G = 1.8250$	$R_G = 0.01820$
$R_a = 0.0015$		

Exciter and Voltage Regulator

$K_A = 50$	$T_E = 0.002$	$T_A = 0.01$

Transmission Line Parameters

$X_t = 0.14$	$R_t = 0.01$	$X_e = 0.56$
$R_e = 0.02$	X_c varies from 0.056 - 0.56 (10% - 100%)	

Governing and Turbine System

$K_g = 25$	$T_1 = 0.2$	$T_2 = 0$
$T_3 = 0.3$	$T_{CH} = 0.3$	$T_{RH} = 7.0$
$T_{CO} = 0.2$	$F_{HP} = 0.3$	$F_{IP} = 0.26$
$F_{LP1} = 0.22$	$F_{LP2} = 0.22$	F

Stabilizer parameters

$K_s = 20$	$T = 3.0$	$T_x = 0.125$
$T_y = 00.05$		

	20%	30%	50%
Shaft modes	-0.1817 ± j298.18	-0.1818 ± j298.18	-0.1818 ± j298.18
	-0.2104 ± j203.20	+0.1541 ± j204.35	+0.1560 ± j202.68
	-0.2266 ± j160.66	-0.2496 ± j160.72	+0.9100 ± j161.42
	-0.6679 ± j127.03	-0.6706 ± j127.03	-0.6799 ± j127.08
	-0.2660 ± j 99.13	-0.2877 ± j 99.21	-0.3545 ± j 99.79
Stator/Network	-6.9800 ± j512.30	-7.0224 ± j542.80	-7.0800 ± j591.15
	-6.0717 ± j241.01	-6.1984 ± j209.20	-6.8387 ± j161.47
Synchronous Machine Rotor	-8.5681	-8.4404	-8.1277
	-31.578	-31.920	-32.808
	-25.397	-25.404	-25.423
	-2.0196	-1.9830	-1.9070
Exciter and Voltage Regulator	-499.98	-499.97	-499.97
	-101.97	-101.91	-101.76
$\lambda\ \delta\ \omega$	+0.0415 ± j8.0234	-0.0479 ± j8.4801	-0.2674 ± j9.5459
Turbine and Governor	-0.1416	-0.1417	-0.1418
	-4.6679	-4.6160	-4.0496
	-2.9271	-3.0336	-3.3335
	-4.7039 ± j0.7567	-4.6732 ± j0.6269	-4.7939 ± j0.3198

Table 3.2 Eigenvalues of SSR model at different degrees of capacitor compensation without conventional stabilizer for P = 0.9 p.u. at 0.9 power factor lagging.

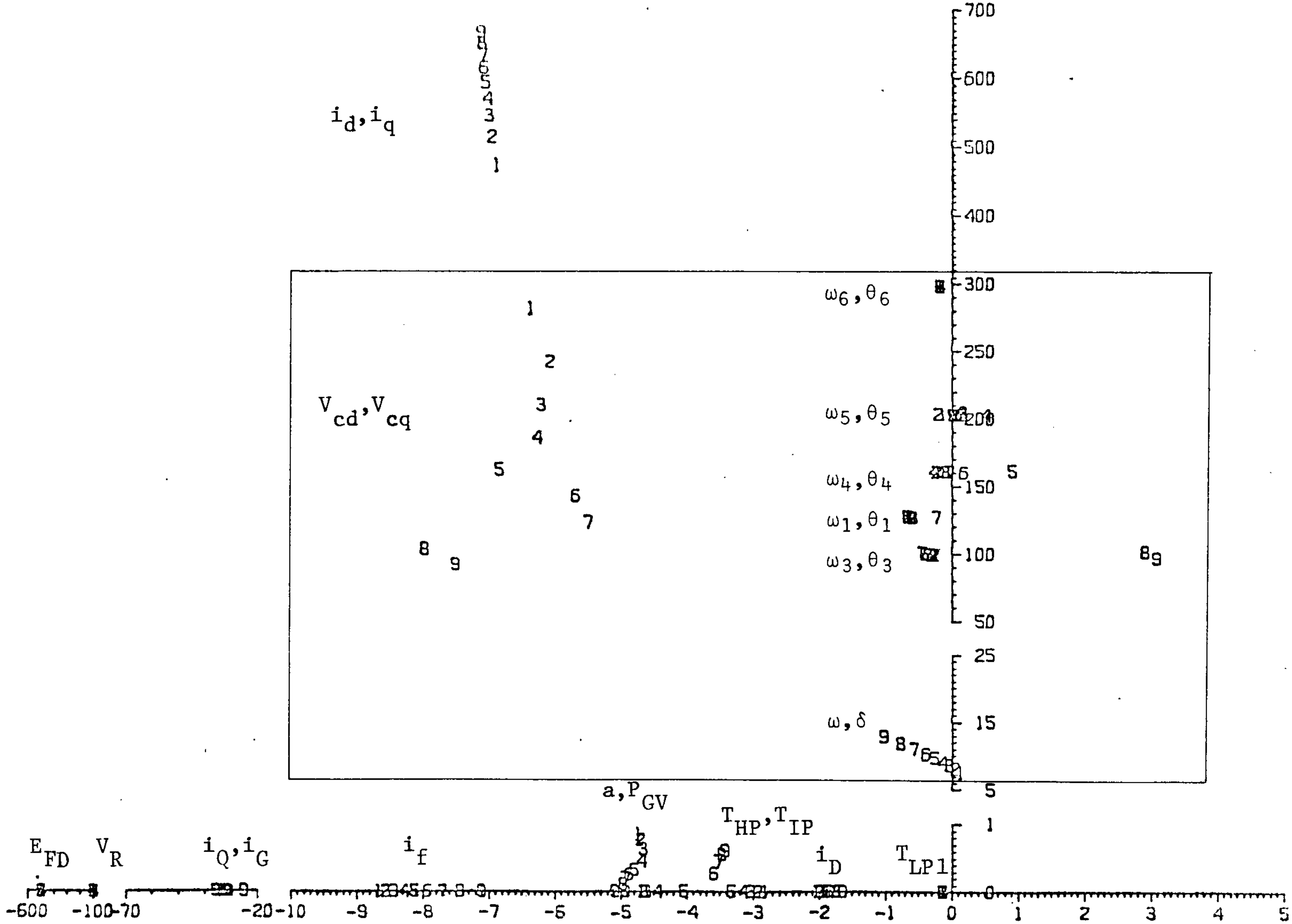

Fig. 3-1 The effect of capacitor compensation without stabilizer for P = 0.9 p.u. at 0.9 power factor lagging.
(The symbols 1,2,3,...9 respectively correspond to 10,20,30,...90% compensation)

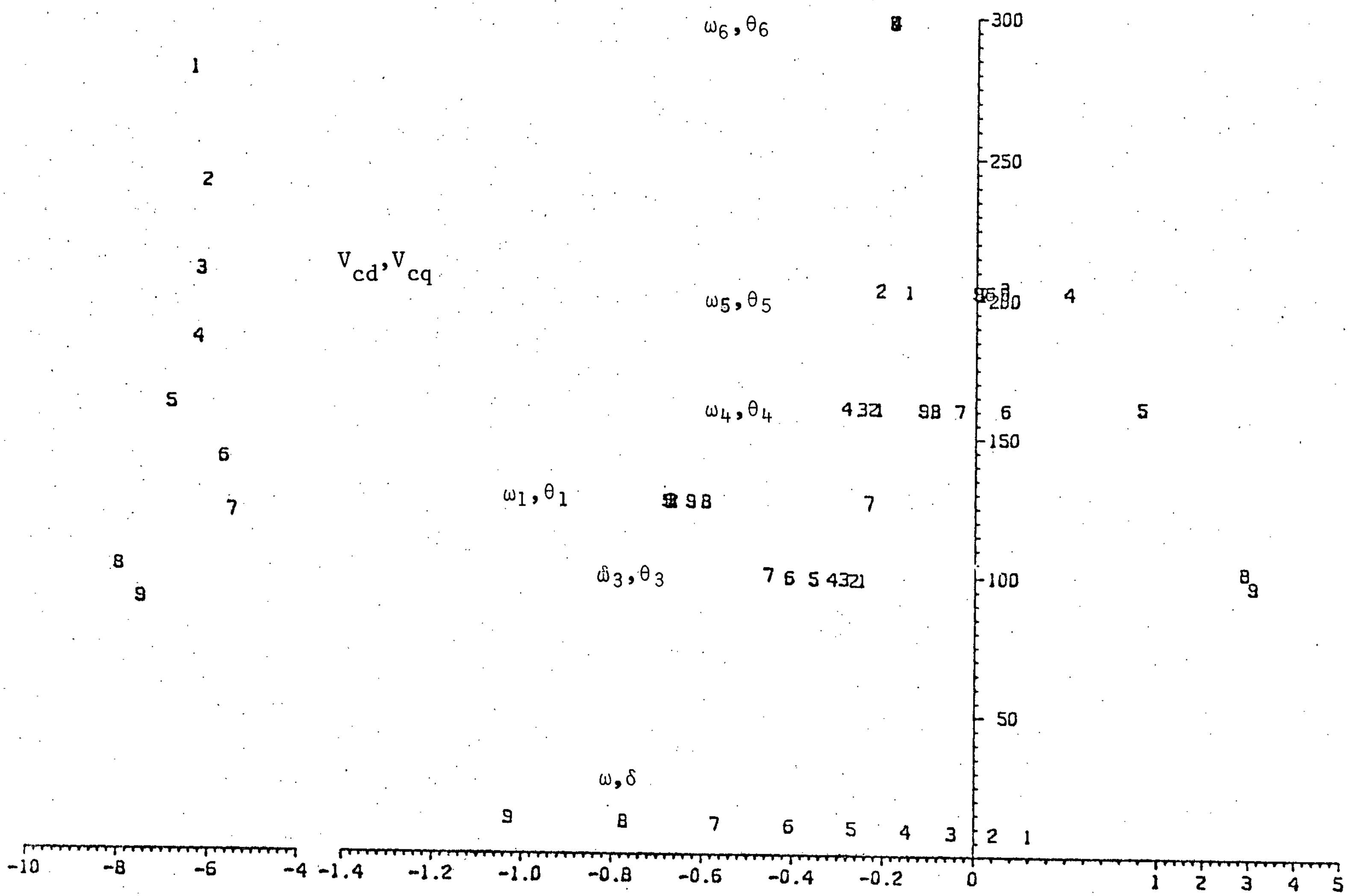

Fig. 3-2 Enlarged portion of Fig. 3-1.
(The symbols 1,2,3,...9 respectively correspond to 10,20,30,...90% compensation)

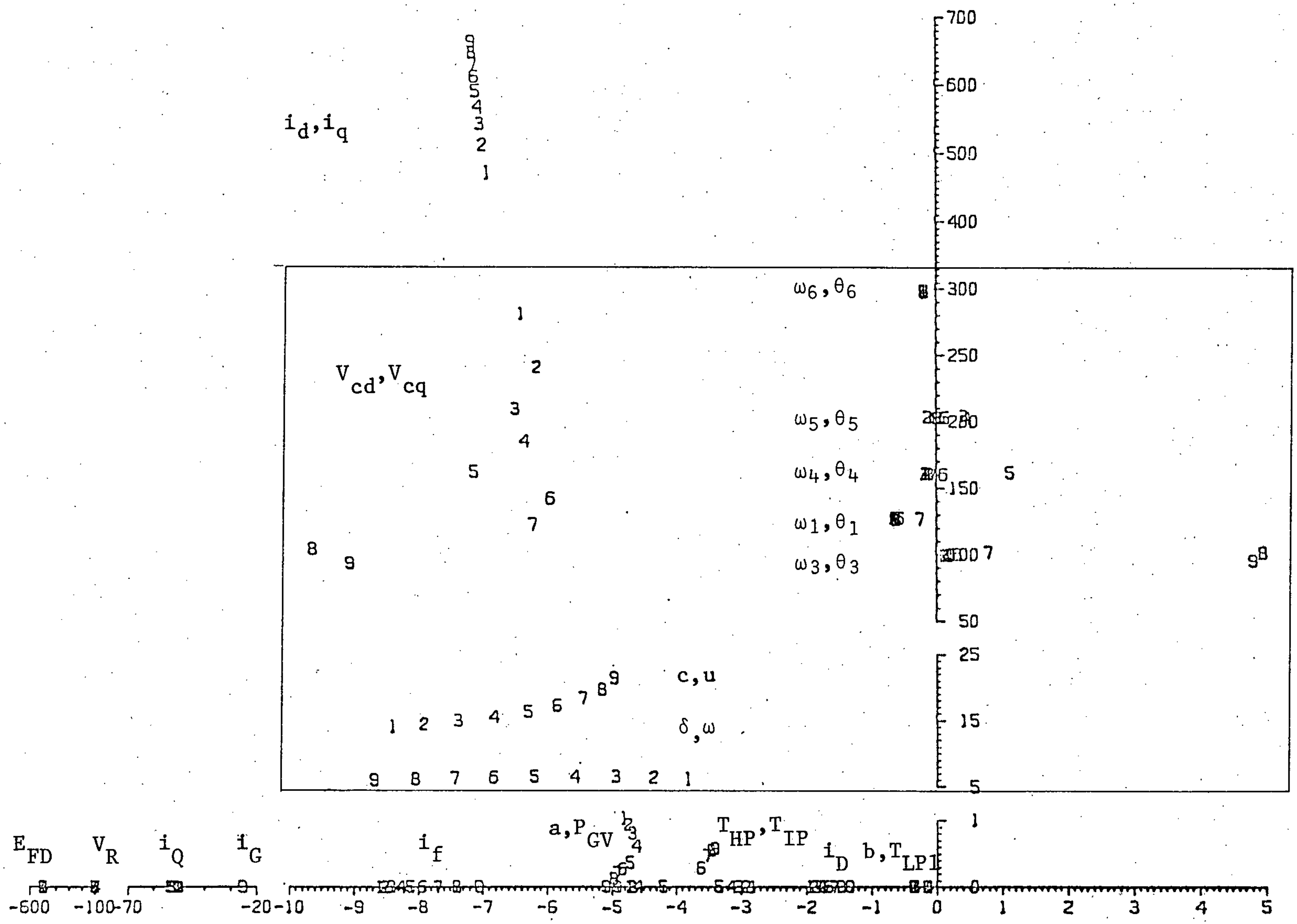

Fig. 3-3 The effect of capacitor compensation with stabilizer for P = 0.9 p.u. at 0.9 power factor lagging.
(The symbols 1,2,3...9 respectively correspond to 10,20,30...90% compensation)

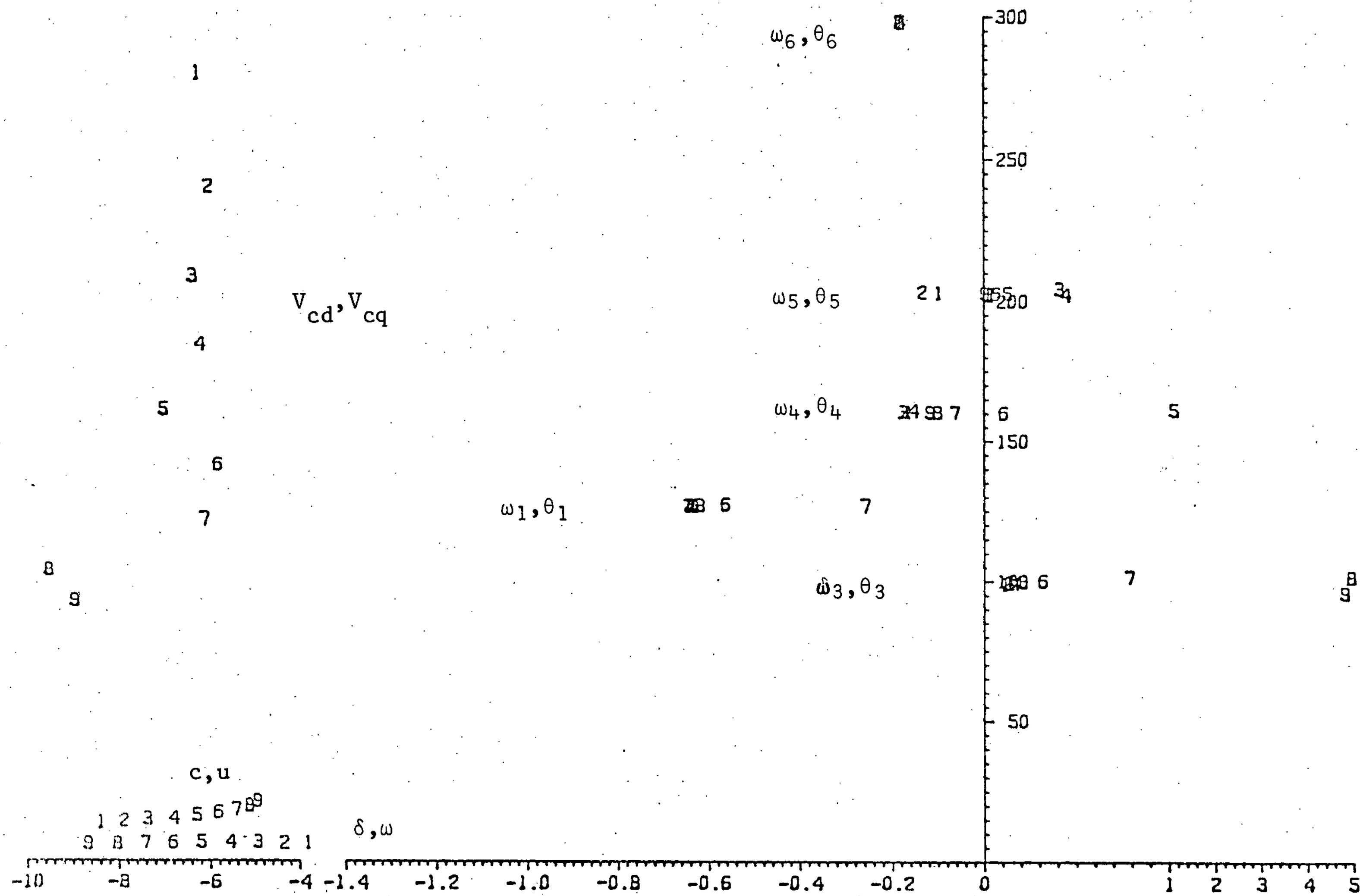

Fig. 3-4 Enlarged portion of Fig. 3-3
(The symbols 1,2,3,...9 respectively correspond to 10,20,30...90% compensation)

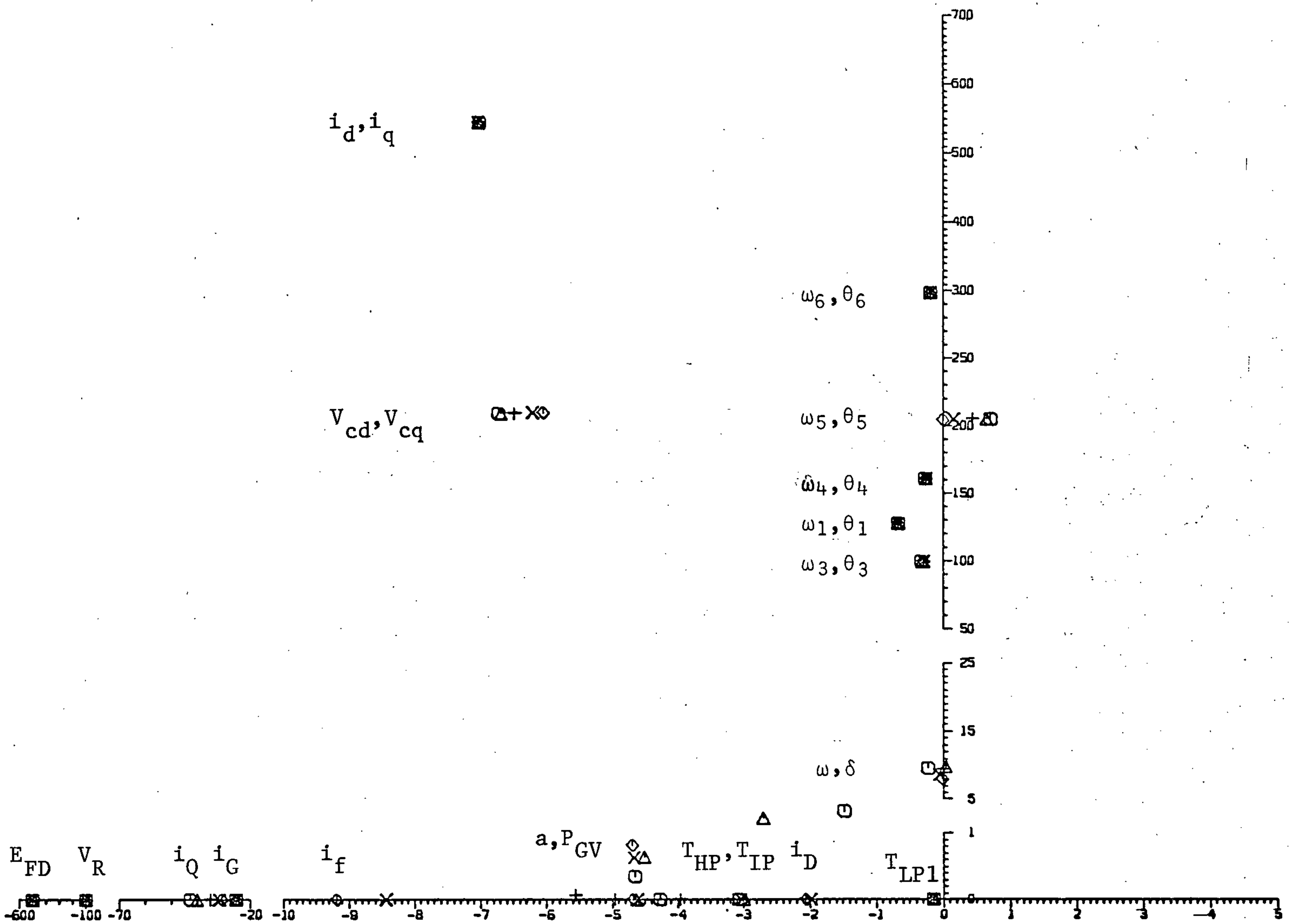

Fig. 3-5 The effect of loading without stabilizer

(The symbols ⊖ = 0.8 p.f. leading, △ = 0.9 p.f. leading, + = unity power factor
X = 0.9 p.f. lagging, ◇ = 0.8 p.f. lagging)

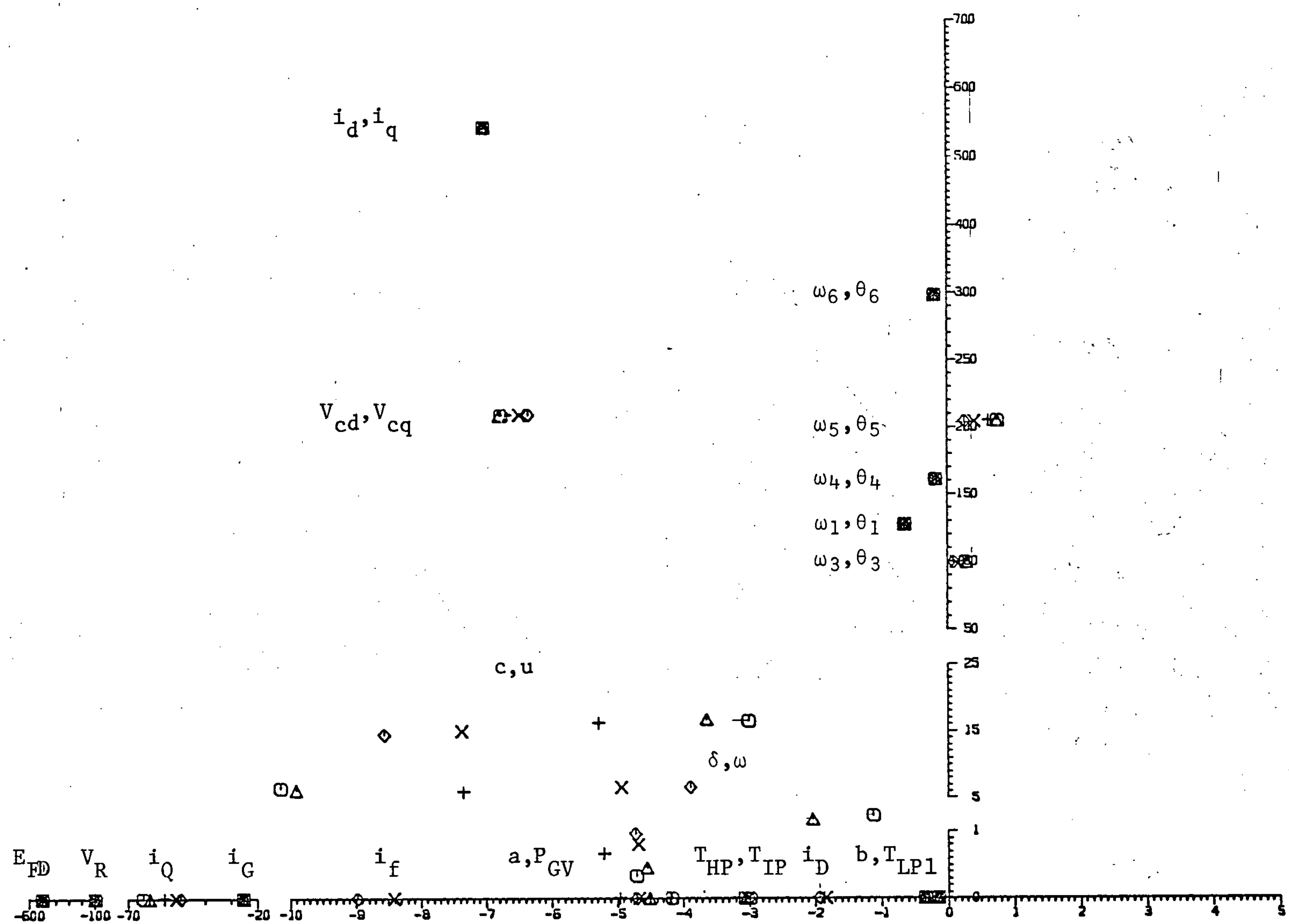

Fig. 3-6 The effect of loading with stabilizer

(The symbols ⊡ = 0.8 p.f. leading, △ = 0.9 p.f. leading, + = unity power factor
X = 0.9 p.f. lagging, ◇ = 0.8 p.f. lagging)

	original system	damper impedance x 0.6	damper impedance x 1.5
Shaft modes	-0.1818 ± j298.18	-0.1818 ± j298.18	-0.1818 ± j298.18
	-0.0288 ± j202.87	-0.0296 ± j202.87	-0.0278 ± j202.87
	-0.1536 ± j160.52	-0.1543 ± j160.52	-0.1528 ± j160.52
	-0.6521 ± j126.98	-0.6522 ± j126.98	-0.6518 ± j126.98
	-0.0238 ± j 98.47	-0.0285 ± j 98.50	-0.0163 ± j 98.42
Stator/Network	-7.1913 ± j715.78	-7.1841 ± j718.50	-7.1873 ± j712.71
	+0.3604 ± j 37.21	-0.2149 ± j 30.47	+0.9064 ± j 42.09
Synchronous Machine Rotor	-5.8109	-5.1370	-7.2552
	-43.39	-31.63	-55.88
	-25.60	-25.51	-25.72
	-0.5040	-0.4187	-0.5597
Exciter and Voltage Regulator	-499.96	-499.98	-499.94
	-100.68	-100.43	-100.95
$\lambda\ \delta\ \omega$	-3.8086 ± j 20.07	-4.1469 ± j 23.81	-3.7030 ± j 18.24
Turbine Governor	-0.1406	-0.1404	-0.1407
	-4.1296	-4.8816	-3.8373
	-3.1202	-3.0225	-3.1684
	-4.5440 ± j0.1525	-3.7438 ± j-.5651	-4.7916 ± j-.2688

Table 3.3 Effect of Damper Winding in zero total reactance and P = 0.9 p.u. at 0.9 power factor lagging.

4. MULTI-MODE TORSIONAL OSCILLATIONS STABILIZATION WITH LINEAR OPTIMAL CONTROL

Linear optimal control theory has been applied to the stabilizer design of power systems [23,8,24]. For practical applications, the state variables used in the design must be measurable. Another problem of optimal control design is the choice of the weighting matirices Q and R in the cost index. A simple procedure was proposed [8] which requires thesstate equations in the canonical form. The Q/R ratio in the procedure can be judiciously chosen.

4.1 State Equations With Measurable Variables

The state equations of the system was written in Chapter 2 in the form

$$\dot{X} = A\,X + Bu \tag{4-1}$$

where A was given as (2-39). For an excitation control,

$$B = [0\ 0\ 0\ \ldots\ 0\ \frac{K_A}{T_A}]^t \tag{4-2}$$

as in (2-31). Let

$$Z = M\,X \tag{4-3}$$

where Z is the measurable variable vector. Then

$$\dot{Z} = M\,X = M\,A\,M^{-1}\,Z + M\,B\,u$$

or

$$\dot{Z} = F\,Z + G\,u \tag{4-4}$$

where $F = M\,A\,M^{-1}$ and $G = M\,B$

Assume that all mechanical system variables, such as angles and speeds of every turbine rotor and that of generator and exciter; torques output from each stage of turbine and governor system and the electrical system variables such as generator power and current, voltage across the capacitor and to ground (generator side), damper currents and voltage output from voltage regulator and exciter , are measurable, then we have

For electrical power

$$\Delta P = V_{do}\,\Delta i_d + V_{qo}\,\Delta i_q + i_{do}\,\Delta V_d + i_{qo}\,\Delta V_q \tag{4-5}$$

By substituting V_d, V_q from equation (2-25)

$$\Delta P = m_{11}\,\Delta i_d + m_{12}\,\Delta i_q + m_{14}\,\Delta V_{cd} + m_{15}\,\Delta V_{cq} + m_{16}\,\Delta\delta \tag{4-6}$$

where $m_{11} = V_{do} + (R_e+R_t)i_{do} + (X_e+X_t)i_{qo}$

$m_{12} = V_{qo} - (X_e+X_t)i_{do} + (R_e+R_t)i_{qo}$

$m_{14} = i_{do}$

$m_{15} = i_{qo}$

$m_{16} = V_o[i_{do}\cos\delta - i_{qo}\sin\delta]$

For terminal current

$$\Delta i_t = \frac{i_{do}}{i_{to}}\,\Delta i_d + \frac{i_{qo}}{i_{to}}\,\Delta i_q \tag{4-7}$$

or $\Delta i_t = m_{21}\,\Delta i_d + m_{22}\,\Delta i_q$

where $m_{21} = \dfrac{i_{do}}{i_{to}}$, $m_{22} = \dfrac{i_{qo}}{i_{to}}$

For voltage across the capacitor

$$\Delta V_{ct} = \frac{V_{cdo}}{V_{co}}\,\Delta V_{cd} + \frac{V_{cqo}}{V_{co}}\,\Delta V_{cq} \tag{4-8}$$

or $\Delta V_c = m_{44}\Delta\Delta V_{cd} + m_{45}\,\Delta V_{cq}$

where $m_{44} = \dfrac{V_{cdo}}{V_{co}}$, $m_{45} = \dfrac{V_{cqo}}{V_{co}}$

For voltage at the terminal of the capacitor.

As shown in Fig. 2-7, V_{ct} is the voltage at the generator side of the capacitor with respect to ground

$$\Delta V_{ct} = \frac{V_{ctdo}}{V_{cto}} \Delta V_{ctd} + \frac{V_{ctqo}}{V_{cto}} \Delta V_{ctq} \qquad (4\text{-}9)$$

where V_{ctd} and V_{ctq} are the d, q components of V_{ct} and can be expressed in terms of the voltage across the capacitor and infinite bus voltages.

$$\Delta V_{ctd} = \Delta V_{cd} + V_o \cos\delta \, \Delta\delta \qquad (4\text{-}10)$$

$$\Delta V_{ctq} = \Delta V_{cq} - V_o \sin\delta \, \Delta\delta$$

or

$$\Delta V_{ct} = m_{54}\, \Delta V_{cd} + m_{55}\, \Delta V_{cq} + m_{56}\, \Delta\delta \qquad (4\text{-}11)$$

where

$$m_{54} = \frac{V_{ctdo}}{V_{cto}}, \qquad m_{55} = \frac{V_{ctqo}}{V_{cto}}$$

$$m_{56} = [V_{ctdo} \cos\delta - V_{ctqo} \sin\delta] \frac{V_o}{V_{cto}}$$

Besides m_{11}, m_{22}, m_{44} and m_{55}, the other main diagonal elements are unity. Other off-diagonal elements are zero except those already derived.

4.2 State Equations in Canonical Form

A design procedure has been developed utilising state equations in canonical form [8]:

$$F_o = \begin{bmatrix} 0 & 1 & \cdot & \cdot & \cdot & 0 \\ \cdot & 0 & 1 & & & \cdot \\ \cdot & & & \ddots & & \cdot \\ \cdot & & & & \ddots & \cdot \\ \cdot & & & & 1 & \cdot \\ 0 & \cdot & \cdot & \cdot & 0 & 1 \\ -\alpha_1 & -\alpha_2 & \cdot & \cdot & -\alpha_{n-1} & -\alpha_n \end{bmatrix} \qquad (4\text{-}12)$$

Let $Z = T\,Y$ (4-13)

we shall have

$$\dot{Y} = T^{-1} \dot{Z} = F_o Y + G_o U \tag{4-14}$$

where $$F_o = T^{-1} F T \tag{4-15}$$

and $$G_o = T G = [0\ 0\ 0\ \dots\ 1]^t \tag{4-16}$$

The transformation matrix T can be found as follows:

Since the eigenvalues remain unchanged with similarity transformation, we shall have

$$|\lambda I - F| = (\lambda-\lambda_1)(\lambda-\lambda_2) \dots (\lambda-\lambda_n) = 0 \tag{4-17}$$

and

$$|\lambda I - F_o| = \lambda^n + \alpha_n \lambda^{n-1} + \alpha_{n-1}\lambda^{n-2} + \dots + \alpha_1 = 00 \tag{4-18}$$

where $\lambda_1, \lambda_2, \dots \lambda_n$ are the eigenvalues of the system. The α's can be determined from (4-16) and (4-17),

$$\alpha_n = -\sum_{i=1}^{n} \lambda_i$$

$$\alpha_{n-1} = \lambda_1\lambda_2 + \lambda_1\lambda_3 + \dots + \lambda_2\lambda_3 + \dots + \lambda_{n-1}\lambda_n$$

$$\alpha_{n-2} = -\lambda_1\lambda_2\lambda_3 - \lambda\lambda_1\lambda_2\lambda_4 - \dots - \lambda_{n-2}\lambda_{n-1}\lambda_n$$

$$\vdots$$

$$\alpha_1 = (-1)^n \prod_{i=1}^{n} \lambda_i \tag{4-19}$$

Let the transformation T matrix be written as

$$T = [T_1, T_2, T_3, \dots T_n] \tag{4-20}$$

where $T_1, T_2, T_3, \dots T_n$ are the column vectors of T matrix. From (4-15) and (4-20), we have

$$T F_o = F T$$ (

or $$[T_1, T_2, T_3, \ldots T_n]\, F_o = F[T_1, T_2, T_3, \ldots T_n] \qquad (4\text{-}21)$$

From (4-16) and (4-21), we have

$$T_n = G \qquad (4\text{-}22)$$

Hence, we can compute T_1, T_2, T_3 ... T_n by using the following recursive formula

$$T_{n-i} = FT_{n-i+1} + \alpha_{n-i+1}\, G \qquad i = 1, 2, 3, \ldots n-1 \qquad (4\text{-}23)$$

and

$$F\, T_1 + \alpha_1 G = 0 \qquad (4\text{-}24)$$

The condition of (4-24) may not be met due to the accumulated computation errors. Let T_1, T_2, T_3, ... T_n be the computed results and $\hat{T}_1$, $\hat{T}_2$, $\hat{T}_3$, ... $\hat{T}_n$ be correct values

$$F\, \hat{T}_1 + \alpha_1\, G = 0$$

$$F\, T_1 + \alpha_1\, G = \varepsilon \qquad (4\text{-}25)$$

and the error

$$\hat{T}_1 - T_1 \triangleq n_1 \qquad (4\text{-}26)$$

Then $$n_1 = -F^{-1}\, \varepsilon \qquad (4\text{-}27)$$

Similarly,

$$F\, \hat{T}_2 + \alpha_2\, G = \hat{T}_1$$

$$F\, T_2 + \alpha_2\, G = T_1 \qquad (4\text{-}28)$$

and $$n_2 = F^{-1} n_1 \qquad (4\text{-}29)$$

Therefore,

$$n_i = F^{-1}\, n_{i-1} \qquad i = 2, 3, 4, \ldots n \qquad (4\text{-}30)$$

$$\hat{T}_i = n_i + T_i$$

4.3 Linear Optimal Control Design

The system equations in canonical form were

$$\dot{Y} = F_o Y + G_o U \tag{4-14}$$

The characteristic equation of the open loop system is

$$|\lambda I - F_o| = \lambda^n + \alpha_n \lambda^{n-1} + \alpha_{n-1}\lambda^{n-2} + \ldots + \alpha_1 \tag{4-31}$$

Let the desired eigenvalues of the closed-loop system be $\hat{\lambda}_1, \hat{\lambda}_2, \hat{\lambda}_3, \ldots \hat{\lambda}_n$

The new characteristic equation will be

$$(\lambda - \hat{\lambda}_1)(\lambda - \hat{\lambda}_2)(\lambda - \hat{\lambda}_3) \ldots (\lambda - \hat{\lambda}_n)$$

$$= \lambda^n + \hat{\alpha}_n \lambda^{n-1} + \hat{\alpha}_{n-1}\lambda^{n-2} + \ldots + \hat{\alpha}_1 = 0 \tag{4-32}$$

Since characteristic equation of the closed loop system is

$$|\lambda I - (F_o - G_o S_o)|$$
$$= \lambda^n + (\alpha_n + \beta_n)\lambda^{n-1} + (\alpha_{n-1} + \beta_{n-1})\lambda^{n-2} + \ldots + (\alpha_1 + \beta_1)$$
$$= 0 \tag{4-33}$$

where

$$U \triangleq -S_o Y \tag{4-34}$$

Equating (4-32) to (4-33) gives

$$\hat{\alpha}_i - \alpha_i = \beta_i \qquad i = 1, 2, 3, \ldots n \tag{4-35}$$

and $$S_o = [\beta_1, \beta_2, \beta_3, \ldots \beta_n] \tag{4-36}$$

Finally, the linear optimal controller in measurable state variables

$$U \triangleq -S_o Y$$

or

$$U \triangleq -S_o T^{-1} Z \tag{4-37}$$

4.4 Stabilization of SSR

Because of the number of state variables which can be measured, the 22nd order and 19th reduced order models are used for the linear optimal control design. Eigenvalue analysis shows that all the important mechanical and electrical eigenvalues are essentially unchanged; Table 4-1.

Single mechanical mode stabilization

At 30% compensation and 0.9 power factor lagging of the reduced 22nd order system without stabilizer, the 204 rad./sec. or 32.5 hertz mechanical mode is excited and has negative damping (eigenvalues with positive real part). By utilizing the design procedure described in this chapter, an optimal controller can be designed to shift the eigenvalues from $+0.1541 \pm j204.35$ to $-6.500 \pm j204.35$ and another mechanical mode which is barely stable from $-0.08805 \pm j8.4938$ to $-6.000 \pm j8.4938$. All eigenvalues are stabilized as shown in Table 4-2. The controller is 7.8 $(7.823\Delta\omega_1,\ 0.0964\Delta\theta_1,\ -183.005\Delta\omega,\ -8.801\Delta\delta,\ 192.487\Delta\omega_3,\ -3.398\Delta\theta_3,\ 65.534\Delta\omega_4,\ 7.448\Delta\theta_4,\ -1.336\Delta\theta_5,\ -47.478\Delta\omega_6,\ -2.738\Delta\theta_6,\ -29.746\Delta P,\ 28.645\Delta i_t,\ 1.454\Delta i_f,\ 1.475\Delta i_D,\ -5.931\Delta i_Q,\ -5.929\Delta i_G,\ -60.094\Delta V_c,\ 35.987\Delta V_{c_t},\ -0.000260\Delta V_R,\ -0.00259\Delta E_{FD})$.

Stabilization of two mechanical modes simultaneously

For the same system but with 50% compensation, two mechanical modes were excited $+0.1560 \pm j202.68$ and $+0.9101 \pm j161.42$ were excited simultaneously. Another optimal controller is designed to shift the two mechanical modes to $-6.500 \pm j202.68$ and $-3.500 \pm j161.42$ as shown in Table 4-3. The controller is $(1.124\Delta\omega_1,\ -4.959\Delta\theta_1,\ -23.848\Delta\omega,\ 189.462\Delta\delta,\ 13.843\Delta\omega_3,\ -321.301\Delta\theta_3,\ 24.286\Delta\omega_4,\ 147.568\Delta\theta_4,\ -6.018\Delta\omega_5,\ 4.467\Delta\theta_5,\ -9.927\Delta\omega_6,\ -25.064\Delta\theta_6,\ -26.719\Delta P,\ 29.533\Delta i_t,\ -1.030\Delta i_f,\ -1.007\Delta i_D,\ -6.711\Delta i_Q,\ -6.712\Delta i_G,\ -22.422\Delta V_c,\ 31.169\Delta V_{c_t},\ -0.000278\Delta V_R,\ -0.00264\Delta E_{FD})$.

Low Order Stabilization Design

Although the two controllers designed by the procedure presented in this chapter have been proved to be effective in stabilizing the system, the damper currents are not directly measurable. Still another linear optimal controller is designed for the system, without the need for damper currents. The equations associated with the damper windings are dropped, resulting in a 19th order system. The controller is ($1.84\Delta\omega_1$, $1.01\Delta\theta_1$, $-41.51\Delta\omega$, $-30.63\Delta\delta$, $54.51\Delta\omega_3$, $39.93\Delta\theta_3$, $7.37\Delta\omega_4$, $-5.77\Delta\theta_4$, $-6.41\Delta\omega_5$, $-3.32\Delta\theta_5$, $-7.46\Delta\omega_6$, $-2.16\Delta\theta_6$, $-1.66\Delta P$, $2.63\Delta i_t$, $-0.872\Delta i_f$, $-2.26\Delta V_c$, $-2.35\Delta V_{tc}$, $-0.000295\Delta V_R$, $-0.00274\Delta E_{FD}$), and the eigenvalues of the system with and without the controller are shown in Table 4-4. Finally the controller is tested on the original system for various degrees of compensation. The results are plotted in Fig. 4-1. It is found that the controller designed for the 19th order model with 30% compensation, not only can stabilize the original 27th order system for 30% compensation but also can stabilize the original system from 10 to 70% compensation. This proves the effectiveness of such controller design in wide-range-compensation multi-mode SSR stabilization.

	original system	reduced 22nd model	reduced 19th model
Shaft modes	-0.1818 ± j298.18	-0.1818 ± j298.18	-0.1818 ± j298.18
	+0.1541 ± j204.35	+0.1541 ± j204.35	-0.2290 ± j203.22
	-0.2496 ± j160.72	-0.2496 ± j160.72	-0.2273 ± j160.66
	-0.6706 ± j127.03	-0.6706 ± j127.03	-0.6677 ± j127.03
	-0.2877 ± j 99.21	-0.2877 ± j 99.21	-0.2627 ± j 99.14
λ δ ω	-0.0479 ± j8.4801	-0.0881 ± j8.4938	-0.2266 ± j7.9054
Stator/Network	-7.0224 ± j542.80	-7.0224 ± j542.80	-4.8208 ± j514.02
	-6.1984 ± j209.20	-6.1984 ± j209.20	-3.6580 ± j238.75
Synchronous Machine Rotor	-8.4404	-8.4858	-8.0056
	-31.920	-31.920	
	-25.404	-25.404	
	-1.9830	-2.1855	
Exciter and Voltage Regulator	-499.97	-499.97	-499.52
	-101.91	-101.91	-93.682
Turbine and Governor	-0.1417		
	-4.6160		
	-3.0336		
	-4.6732 ± j0.6269		

Table 4-1 Eigenvalues of original system and reduced order models without controller at 30% compensation and P = 0.9 p.u. at 0.9 power factor lagging.

	reduced 22nd order model without controller	reduced 22nd order model with controller	original system with controller
Shaft modes	-0.1818 ± j298.18	-0.1818 ± j298.18	-0.1818 ± j298.18
	+0.1541 ± j204.35	-6.5000 ± j204.35	-6.5000 ± j204.35
	-0.2496 ± j160.72	-3.5000 ± j160.72	-3.5000 ± j160.72
	-0.6706 ± j127.03	-0.6706 ± j127.03	-0.6706 ± j127.03
	-0.2877 ± j 99.21	-0.2877 ± j 99.21	-0.2877 ± j 99.21
λ δ ω	-0.0881 ± j8.4938	-6.0000 ± j8.4938	-6.2367 ± j8.4158
Stator/Network	-7.0224 ± j542.80	-7.0224 ± j542.80	-7.0224 ± j542.80
	-6.1984 ± j209.20	-6.1984 ± j209.20	-6.1984 ± j209.20
Synchronous Machine Rotor	-8.4858	-8.4858	-9.6038
	-31.920	-31.920	-31.923
	-25.404	-25.404	-25.404
	-2.1855	-2.1855	-1.5570
Exciter and Voltage Regulator	-499.97	-499.97	-499.97
	-101.91	-200.00	-200.00
Turbine and Governor			-0.1404
			-4.8741
			-2.8538
			-3.9883 ± j2.9898

Table 4-2 Eigenvalues of reduced 22nd order model with/without controller and original system with the controller at 30% compensation and P = 0.9 p.u. at 0.9 power factor lagging.

	reduced 22nd order model without controller	reduced 22nd order model with controller	original system with controller
Shaft modes	-0.1818 ± j298.18	-0.1818 ± j298.18	-0.1818 ± j298.18
	+0.1560 ± j202.68	-6.5000 ± j202.68	-6.5000 ± j202.68
	+0.9101 ± j161.42	-3.5000 ± j161.42	-3.5000 ± j161.42
	-0.6799 ± j127.08	-0.6799 ± j127.08	-0.6799 ± j127.08
	-0.3545 ± j 99.49	-0.3545 ± j 99.49	-0.3545 ± j 99.49
λ δ ω	-0.2958 ± j9.5621	-6.0000 ± j9.5621	-6.4682 ± j9.7544
Stator/Network	-7.0799 ± j591.16	-7.0799 ± j591.15	-7.0799 ± j591.15
	-6.8387 ± j161.47	-6.8387 ± j161.47	-6.8387 ± j161.47
Synchronous Machine Rotor	-8.1783	-8.1783	-10.953
	-32.808	-32.808	-32.793
	-25.423	-25.423	-25.424
	-2.1030	-2.1030	-1.0891
Exciter and Voltage Regulator	-499.97	-499.97	-499.97
	-101.76	-200.00	-200.00
Turbine and Governor			-0.1384
			-4.8909
			-3.1454
			-2.9767 ± j4.0177

Table 4-3 Eigenvalues of reduced 22nd order model with/without controller and original system with the controller at 50% compensation and P = 0.9 p.u. at 0.9 power factor lagging.

	reduced 19th order model without controller	reduced 19th order model with controller	original system with controller
Shaft modes	-0.1818 ± j298.18	-0.1817 ± j298.18	-0.1818 ± j298.18
	-0.2290 ± j203.22	-6.5000 ± j203.22	-0.4968 ± j203.19
	-0.2273 ± j160.66	-3.5000 ± j160.66	-0.2790 ± j160.52
	-0.6677 ± j127.03	-0.6676 ± j127.03	-0.6697 ± j127.04
	-0.2627 ± j 99.14	-0.2628 ± j 99.14	-0.2770 ± j 99.22
λ δ ω	-0.2266 ± j7.9054	-6.0000 ± j7.9054	-0.1092 ± j8.7874
Stator/Network	-4.8208 ± j514.02	-4.8208 ± j514.02	-7.1255 ± j542.54
	-3.6580 ± j238.75	-3.6582 ± j238.75	-5.9600 ± j209.43
Synchronous Machine Rotor	-8.0056	-8.0056	-25.4025
			-2.8136 + j0.2572
			-2.8136 - j0.2572
			-1.6473 + j391.91
Exciter and Voltage Regulator	-499.52	-499.52	-773.59
	-93.682	-200.00	-1.6473 - j391.91
Turbine and Governor			-0.1401
			-4.6414
			-0.2592
			-4.7914 ± j0.9552

Table 4-4 Eigenvalues of reduced order model with/without controller and original system with the controller at 30% compensation and P = 0.9 p.u. at 0.9 power factor lagging.

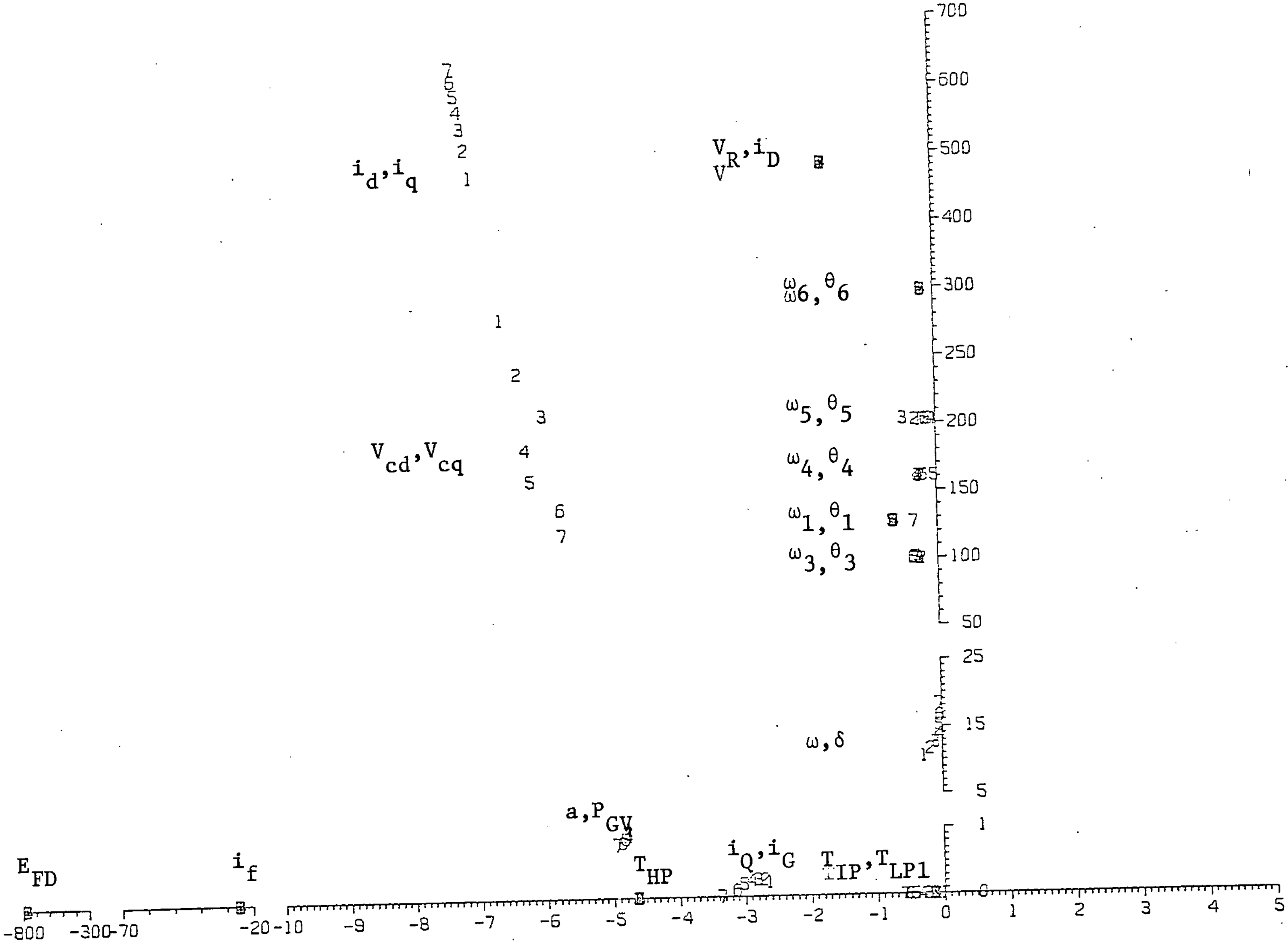

Fig. 4-1 The effect of capacitor compensation with controller for P = 0.9 p.u. at 0.9 power factor lagging.
(The symbols 1,2,3,...7 respectively correspond to 10,20,30,...70% compensation)

5. CONCLUSIONS

A high-order power system model for subsynchronous resonance studies is developed. The model includes mass-spring system, synchronous machine, series capacitor compensated transmission lines, turbines and governor, voltage regulator and exciter. The transient terms $p\psi_d$ and $p\psi_q$ are included.

From eigenvalue analysis, it is found that by changing the degree of compensation the frequency of the electrical mode will be changed and that, in some cases, even more than one mechanical mode can be excited at the same time. When a conventional lead-lag supplementary excitation control for the stabilization of small oscillations is included, it has an adverse effect on the other mechanical modes close to the small oscillation mode. Such finding is in agreement with other previous work [22]. When the damper impedance is decreased, it does reduce the possibility of SSR under ideal conditions [5].

Linear optimal controllers based upon an earlier developed method [8] are designed. Two controllers are designed with a reduced 22nd order model and one with a reduced 19th order model and the latter controller not only can stabilize the original 27th order system for 30% compensation, but also can stabilize the system for wide-range compensation and multi-mode SSR.

REFERENCES

[1] IEEE Task Force, "Analysis and Control of Subsynchronous Resonance", IEEE Publication 76CH1066-0-PWR, IEEE, New York, 1976.

[2] L.A. Kilgore, L.C. Elliott and E.R. Taylor, "The Prediction and Control of Self-Excited Oscillations due to Series Capacitors in Power Systems", IEEE Transactions on Power Apparatus and Systems, Vol. PAS 90, pp. 1305-1311, May/June 1971.

[3] M.C. Hall and D.A. Hodges, "Experience with 500 KV Subsynchronous Resonance and Resulting Turbine Generator Shaft Damage at Mohave Generating Station", IEEE Publication 76CH1066-0-PWR, pp. 22-25, 1976.

[4] IEEE Committee, "Proposed Terms and Definitions for Subsynchronous Resonance in Series Compensated Transmission Systems", IEEE Publication 76CH1066-0-PWR, pp.55-58, 1976.

[5] R.G. Farmer, A.L. Schwalb and Eli Katz, "Navajo Project Report on Subsynchronous Resonance Analysis and Solutions", IEEE Publication 76CH1066-0-PWR, pp.55-58, 1976.

[6] L.A. Kilgore, D.G. Ramey and M.C. Hall, "Simplified Transmission and Generation Station System Analysis Procedures for Subsynchronous Resonance Problems", IEEE Publication 76CH1066-0-PWR, pp.6-11, 1976.

[7] Colin E.J. Bowler and Donald N. Ewart, "Self-Excited Torsional Frequency Oscillations with Series Capacitors", IEEE Trans. on PAS, Vol. PAS 92, pp. 1688-1695, Sept./Oct. 1973.

[8] B. Habibullah and Yao-Nan Yu, "Physical Realizable Wide Power Range Optimal Controllers for Power Systems", IEEE Trans. on PAS, Vol. 93, pp. 1498-1506, Sept./Oct. 1974.

[9] IEEE Task Force, "Symposium on Adequacy and Philosophy of Modelling: Dynamic System Performance", IEEE Publication 75CH0970-4-PWR, IEEE, New York, 1975.

[10] F.P. deMello, "Power System Dynamics - overview", IEEE Publication 75CH0970-4-PWR, pp. 5-15, 1975.

[11] Charles Concordia and Richard P. Schulz, "Appropriate Component Representation for the Simulation of Power System Dynamics", IEEE Publication 75CH0970-4-PWR, pp. 16-23, 1975.

[12] P.L. Dandeno, "Practical Application of Eigenvalues Techniques in the Analysis of Power System Dynamic Stability Problems", Canadian Electrical Engineering Journal, Vol. 1, No. 1, pp. 35-46, 1976.

[13] W.A. Tuplin, "Torsional Vibration", Pitman, England, 1966.

[14] IEEE Committee Report, "Dynamic Models for Steam and Hydro Turbines in Power System Studies", IEEE Trans. on PAS, Vol. PAS 92, pp. 1904-1915, Nov./Dec. 1973.

[15] W. Janischewskyj and P. Kunder, "Simulation of the Non-Linear Dynamic Response of the Interconnected Synchronous Machines", IEEE Trans. on PAS, Vol. PAS 91, pp. 2064-2077, Sept./Oct. 1972.

[16] P.L. Dandeno, P. Kunder and R.P. Schulz, "Recent Trends and Progress in Synchronous Machine Modeling in the Electric Utility Industry", Proceeding of IEEE, July 1974.

[17] E.W. Kimbark, "Power System Stability", (Vol. III, pp. 57-60), Wiley, New York, 1956.

[18] IEEE Committee Report, "Computer Respresentation of Excitation Systems", IEEE Trans. PAS, Vol. PAS 87, pp. 1460-1470, June/July 1968.

[19] F.P. deMello and C. Concordia, "Concepts of Synchronous Machine Stability as Affected by Excitation Control", IEEE Trans. PAS, Vol. PAS 88, pp. 316-329, Mar./Apr. 1969.

[20] IEEE Task Force, "First Benchmark Model for Computer Simulation of Subsynchronous Resonance", IEEE Publication F 77 102-7.

[21] W. Watson and M.E. Coultes, "Static Exciter Stabilizing Signals on Large Generators - Mechanical Problems", IEEE Trans. PAS, Vol. 92, pp. 204-211, Jan./Feb. 1973.

[22] V.M. Raina, W.J. Wilson and J.H. Anderson, "The Control of Rotor Torsional Oscillations Excited by Supplementary Exciter Stabilization", IEEE Publication A76 457-2.

[23] H.A.M. Moussa and Y.N. Yu, "Optimal Power System Stabilization Trough Excitation and/or Governor Control", IEEE Trans. PAS, Vol. PAS 91, pp. 1166-1174, May/June 1972.

[24] Y.N. Yu, K. Vongsuriya and L.N. Wedman, "Application of an Optimal Control Theory to a Power System", IEEE Trans. PAS, Vol. PAS 89, pp. 55-62, Jan./Feb. 1970.

[25] J.A. Anderson and V.M. Raina, "Power System Excitation and Governor Design Using Optimal Control Theory", Int. Journal of Control, Vol. 12, pp. 289-308, 1972.